Radio-frequency dressed state potentials for neutral atoms

S. Hofferberth,[1,*] I. Lesanovsky,[1,2] B. Fischer,[1] J. Verdu,[1] and J. Schmiedmayer[1,3]

[1] *Physikalisches Institut, Universität Heidelberg, D-69120 Heidelberg, Germany*
[2] *Institute of Electronic Structure and Laser, Foundation for Research and Technology,GR-71110 Heraklion, Greece*
[3] *Atominstitut Österreichischer Universitäten, TU-Wien, Vienna, Austria*

(Dated: February 1, 2008)

Potentials for atoms can be created by external fields acting on properties like magnetic moment, charge, polarizability, or by oscillating fields which couple internal states. The most prominent realization of the latter is the optical dipole potential formed by coupling ground and electronically excited states of an atom with light. Here we present an experimental investigation of the remarkable properties of potentials derived from radio-frequency (RF) coupling between electronic ground states. The coupling is magnetic and the vector character allows to design state dependent potential landscapes. On atom chips this enables robust coherent atom manipulation on much smaller spatial scales than possible with static fields alone. We find no additional heating or collisional loss up to densities approaching 10^{15} atoms / cm^3 compared to static magnetic traps. We demonstrate the creation of Bose-Einstein condensates in RF potentials and investigate the difference in the interference between two independently created and two coherently split condensates in identical traps. All together this makes RF dressing a powerful new tool for micro manipulation of atomic and molecular systems.

PACS numbers: 39.90.+d, 03.75.Be

Dressing of internal states of an atom with an external field is a well known technique in quantum optics [1]. The coupling of atomic states to an oscillating field leads to new eigenstates and eigenenergies in the combined system. These dressed states can form adiabatic potentials, which can be employed for atom trapping and manipulation. The most prominent example is the optical dipole potential [2] created when intense coherent light couples ground and electronically excited states of an atom. To create conservative potentials for coherent manipulation spontaneous relaxation of the excited state has to be avoided and hence the light field has to be far detuned. Consequently the magnitude and shape of the dipole potential is given by the local intensity of the light field. Such far detuned dipole potentials are widely used in ultra cold atom experiments [3].

Dressing can also be achieved by coupling hyperfine components of the electronic ground state by a magnetic radio-frequency (RF) or micro-wave (MW) field. Dressed state potentials resulting from RF coupling of two spin states in a magnetic field have been studied in neutron optics [4]. Adiabatic potentials induced by coupling hyperfine states with a micro wave have been proposed in Ref. [5], and a detuned micro-wave has been used for trapping ultra cold Cs atoms [6]. The trapping of neutral atoms with RF induced potentials was proposed in [7] and first demonstrated for thermal Rb atoms [8]. Recently RF dressed state potentials were employed for coherent splitting of a one-dimensional Bose-Einstein condensate and matter-wave interference [9]. In this paper, we give for the first time a full experimental demonstration and analysis of the remarkable properties of these adiabatic RF dressed state potentials, which make them a versatile new tool for experiments with ultra cold atomic and molecular systems.

*Electronic address: hofferberth@atomchip.org

I. RF DRESSED STATE POTENTIALS

In contrast to the optical dipole potential only electronic ground states are involved in magnetic RF dressing. Consequently there are no spontaneous relaxation processes and conservative potentials can also be created with on-resonant radiation. The coupled states are the magnetic sub-states of an atomic hyperfine ground state and a spatially dependent Zeeman-shift can be used to locally change the coupling strength. Furthermore, the coupling is magnetic and of vector nature, hence not only the amplitudes but also the (local) orientation of the involved RF and static magnetic fields determine the coupling strength [10].

For our experiments we create the RF dressed state potentials by combining a static Ioffe magnetic trap ($\mathbf{B}_S(\mathbf{r})$) with a two component homogeneous RF-field ($\mathbf{B}_{\mathrm{RF}}$) with frequency ω_{RF} and relative phase shift δ.

$$\mathbf{B}_S(\mathbf{r}) = Gx\mathbf{e}_x - Gy\mathbf{e}_y + B_I\mathbf{e}_z \quad (1)$$

$$\mathbf{B}_{\mathrm{RF}} = B_{\mathrm{A}}\mathbf{e}_x\cos(\omega_{\mathrm{RF}}t) + B_{\mathrm{B}}\mathbf{e}_y\cos(\omega_{\mathrm{RF}}t+\delta). \quad (2)$$

G is the gradient of the underlying static quadrupol field and B_{I} the magnitude of the Ioffe field. Following [10] the adiabatic RF-potential created can be written as

$$V = m_F g_F \mu_B \sqrt{\Delta(\mathbf{r})^2 + \Omega_{\mathrm{RF}}(\mathbf{r})^2}. \quad (3)$$

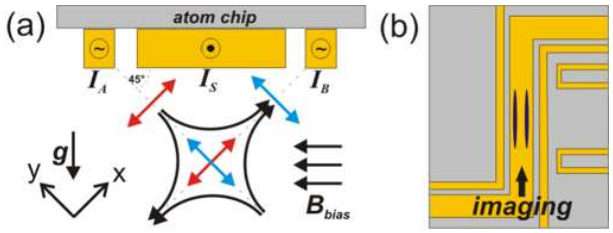

FIG. 1: Atom chip setup for RF-potentials. (a) Side view of the three-wire setup. A broad (100 μm) central wire creates the static trapping potential. Smaller (10 μm) wires on each side provide the oscillating magnetic fields that create the adiabatic RF-potentials. The static trap is positioned so that the two RF-fields are perpendicular at its center. (b) Top view of the atom chip showing the relevant wires. The longitudinal confinement of the static trap is provided by the outer leads of the Z-wire. Additional U-wires on the side can be used to increase this confinement.

with

$$\Delta(\mathbf{r}) = |\mathbf{B}_S(\mathbf{r})| - \frac{\hbar\omega}{|g_F\mu_B|} \quad (4)$$

$$\frac{8\,|\mathbf{B}_S(\mathbf{r})|^2\,\Omega_{\mathrm{RF}}^2(\mathbf{r})}{B_{\mathrm{A}}^2+B_{\mathrm{B}}^2} = 2B_{\mathrm{I}}\left[B_{\mathrm{I}}+|\mathbf{B}_S(\mathbf{r})|\sin(2\alpha)\sin\gamma\right] + G^2\rho^2\left[1-\cos(2\alpha)\cos(2\phi)\right. \quad (5)$$
$$\left. +\sin(2\alpha)\sin(2\phi)\cos\gamma\right].$$

where $\rho=\sqrt{x^2+y^2}$, $\phi=\arctan\frac{y}{x}$ are polar coordinates, $\tan(\alpha)=\frac{B_B}{B_A}$, and $\gamma=-\frac{g_F}{|g_F|}\delta$ is the effective phase shift which depends on the g-factor g_F of the hyperfine manifold under consideration.

II. IMPLEMENTATION ON AN ATOM CHIP

For the experimental realization of RF dressed state potentials, atoms confined in a static magnetic trap have to be irradiated with a radio-frequency field. Atom chips [11] are ideally suited to provide this field, as large field amplitudes can be created by oscillating currents of relatively low amplitude in the chip wires. Additionally, the precise control over the resulting fields and the large field gradients of wire traps allow to fully exploit the possibilities of RF potentials.

In our experiment we use a three-wire atom chip design shown in Fig. 1. A central Z-shaped wire together with an external bias field forms a highly anisotropic Ioffe trap, while the two wires on the sides carry oscillating currents with frequency ω_{RF}. If the static trap is placed at a position from the surface equal to half the distance between the RF wires, the field configuration of two perpendicular RF-fields as discussed above is realized in the vicinity of the trap center. By controlling the phase shift and the amplitudes B_A, B_B of the oscillating fields, we gain full control over the magnitude and polarization of the resulting RF dressing field.

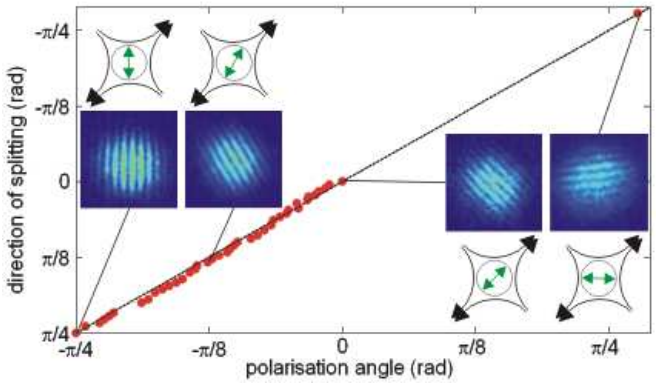

FIG. 2: Orientation of the double well potential as a function of the plane of polarization in the case of a linearly polarized RF field (angles are measured with respect to the x-axis). The double well direction is inferred from interference patterns. The observed fringes are always perpendicular to the double well axis. Coherent splitting is possible in every direction.

Our experiments are performed with Bose-Einstein condensates (BECs) of 10^3 to 10^5 ^{87}Rb atoms. We have $\mu \simeq \hbar\omega_\perp$, where μ is the chemical potential of the BEC, so that we are working in the crossover regime between elongated 3D BEC and 1D-quasi condensates [12, 13].

III. LINEAR RF POLARIZATION

We first discuss the case of a linearly polarized RF dressing field ($\delta = 0, \pi$). The orientation of the polarization is determined by the amplitude ratio $\frac{B_B}{B_A}$. From Eq. (4) it follows that for any orientation, always a double well forms, with the minima located along the direction where the quadrupole component of the static magnetic field is parallel to the RF-field. The dependence of the double well orientation on the field polarization is shown in Fig. 2. We study the double well rotation by observing interference patterns in time-of-flight (ToF) between the matter-wave packets released from the two wells [9].

When rotating the double well, gravity adds an asymmetry of $\Delta U = 2.1389$ [kHz/μm] $\sin\phi$ to the potential. This imbalance quickly becomes strong enough to cause the BEC being trapped solely in the lower well. Symmetric splitting can be achieved by bringing the double well closer to the chip surface. The inhomogeneity of the wire fields also introduces a well controllable asymmetry when shifting the trap location by a few μm, which allows to precisely counteract the effect of gravity. We have observed coherent splitting (the interference shows a stable phase) for all orientations of the double well.

By applying a periodic modulation to the RF amplitudes, such a setup can be used to rotate a BEC on a circular path. The rotation is always centered perfectly on the center of the static trapping potential.

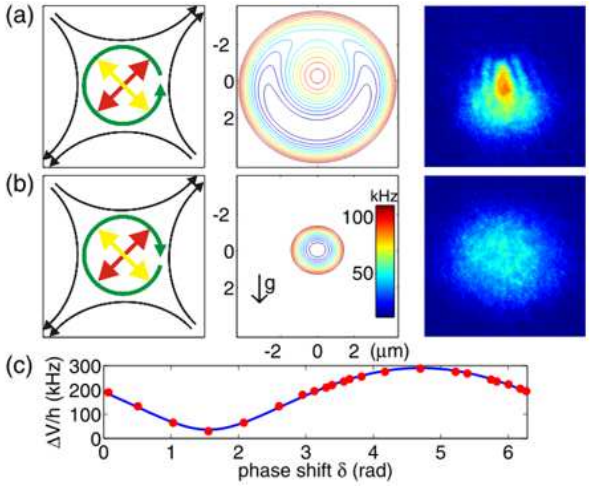

FIG. 3: (a,b) RF-potentials created by circular polarization for Rb in the $F = 2, m_F = 2$ state. Depending on the handedness of the polarization *(left column)* two different potentials result *(center column)*. The potentials shown are numerical calculations for the exact wire geometry used in the experiments, including gravity. The *(right column)* shows the ToF images of BECs released from either configuration.The peculiar interference pattern caused by the deformed ring is clearly visible. *(c)* Measurement of the energy difference between dressed states at the trap bottom for elliptical polarization ($B_B = 1.2 \times B_A$) as a function of the phase shift δ. The line is a numerical calculation for the actual experimental parameters.

IV. ARBITRARY POLARIZATION: STATE DEPENDENT MANIPULATION

A second case of interest is that of circular (or in general elliptical) polarization. For $B_A = B_B$ a phase shift of $\delta = \frac{\pi}{2}$ ($\frac{3\pi}{2}$) leads to right-(left) handed circular polarization. From Eq. (4) one sees that the resulting potentials differ for either case. Depending on the sign of the g-factor one finds a harmonic trap ($\mathrm{sgn}(g_F) = +1$ (-1), $\delta = \frac{\pi}{2}$ ($\frac{3\pi}{2}$)) or a ring potential ($\mathrm{sgn}(g_F) = +1$ (-1), $\delta = \frac{3\pi}{2}$ ($\frac{\pi}{2}$)).

It is interesting to note here that $\mathrm{sgn}(g_F)$ defines an *effective* polarization felt by the atom. In particular, an atom in a hyperfine state with $\mathrm{sgn}(g_F) = -1$ will see the potential formed by the opposite handedness compared to an atom with $\mathrm{sgn}(g_F) = +1$. Consequently, potentials created by circularly, or more generally elliptically, polarized RF can be used for a state-dependent manipulation of trapped atoms.

Fig. 3 illustrates an example of manipulating Rb in the $F = 2, m_F = 2$ state with circular polarized RF. A phase shift of $\delta = \frac{3\pi}{2}$ (Fig. 3a) gives a ring shaped potential, while in the case of $\delta = \frac{\pi}{2}$ (Fig. 3b) the harmonic shape of the static potential is unmodified by the RF-dressing. In the calculation of the resulting potentials as shown in Fig. 3 gravity has been included, and hence the ring is deformed. In our current setup, this deformation can not be fully compensated by changing the static trap and the RF parameters. Nevertheless the time-of-flight images of atoms released from the potentials illustrate the effect caused by the different handedness of the polarization. For $\delta = \frac{\pi}{2}$ the image is identical to that of atoms released from the static trap, while for $\delta = \frac{3\pi}{2}$ we observe an interference pattern which is consistent with numerical simulations of the expansion from the ring potential deformed by gravity. For an ideal ring shaped BEC at T=0 one would expect an interference pattern reminiscent of the poisson spot in optics, with the size of the peak depending on the nonlinear interaction caused by the atom-atom repulsion.

To achieve a perfect ring one would either have to change the orientation of the atom chip resulting in a ring lying in a plane orthogonal to gravity or apply an additional field gradient canceling gravity. This can be achieved for example by an electric field gradient [14].

The effect of the polarization of the RF field on the dressed state potentials can be directly measured by RF spectroscopy of the trapped atoms (Fig. 3c). Thereby we irradiate the dressed BEC with a weak additional RF field. If this RF field is resonant with the energy difference between dressed state levels, atoms are transferred to un-trapped states, and one observes trap loss. We measure the shift of the dressed state potential minimum as a function of the phase shift δ for the case $B_B = 1.2 \times B_A$. The measured potential is in perfect agreement with a numerical calculation based on the actual atom chip dimensions. The dressed state shift varies from ~ 50 kHz at $\delta = \frac{\pi}{2}$ to ~ 320 kHz at $\delta = \frac{3\pi}{2}$.

V. ADVANTAGES IN DESIGNING POTENTIALS

To illustrate the power of RF induced adiabatic potentials for atom manipulation we compare the splitting of a single trap into a double well by RF to the widely discussed splitting based on a 2-wire configuration employing static fields only [11, 15, 16, 17, 18].

First one observes a drastic difference in the topology of the splitting (Fig. 4): In the RF case a single trap smoothly splits into a double well, while in the two wire setup two incoming ports merge and split into two outgoing ports. This potential configuration of the two wire beam splitter [19] and the weak confinement in the splitting region as discussed below are fundamental consequences of Maxwell's equations which constrain the freedom of designing static magnetic potentials [20].

Secondly the overall confinement of the trap during the splitting behaves very differently in either configuration. In the case of static fields the splitting and merging process relies on higher order multi-poles and results in a significantly weaker confinement in *both* transverse directions than in the quadrupole based Ioffe traps at the start and the end of the splitting sequence. In contrast, for the RF potentials the confinement orthogonal to the splitting plane stays nearly constant as can be seen from

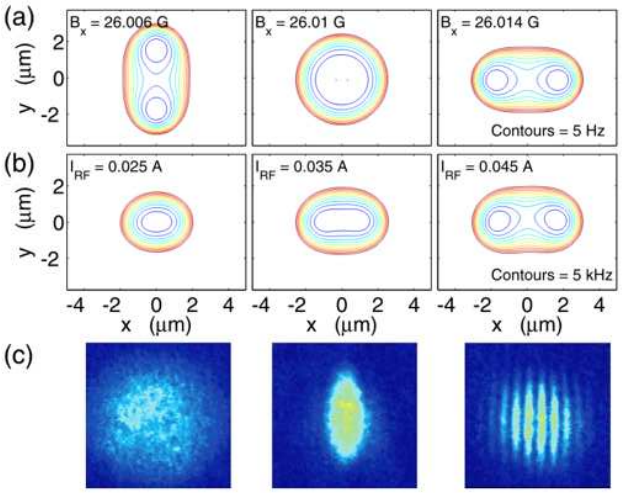

FIG. 4: Comparing double well potentials created with static fields and RF dressing keeping the same structure size and distance to the chip. (a) 2-wire beam splitter: The splitting commences from two incoming guides evolving into two outgoing guides, through a region with a hexapol confinement. Equipotential lines are drawn at steps of 5 Hz. (b) Double well created by RF dressing a single Ioffe trap. The splitting transforms a single trap to a double well. The transverse confinement stays nearly constant and harmonic. At the splitting point one finds a x^4 confinement in the direction of the splitting. Equipotential lines are drawn at steps of 5 kHz. (c) ToF pictures of pure BECs released during the splitting process. *left*: Single BEC from the original static trap. *center*: BEC released at the splitting point. *right*: Interference pattern from the split condensate. The transverse width of the ToF expansion stays constant, illustrating the nearly constant transverse confinement. At the splitting point the narrow width of the ToF image illustrates the reduced confinement in the direction of the splitting.

the ToF images in Fig. 4c.

The difference between the two splitting methods can best be quantified by approximating the symmetric double well by a generic polynomial potential of the form

$$V_{\mathrm{DW}} = bx^2 + dx^4 \tag{6}$$

where the coefficients b and d determine the potential shape. If $b > 0$ there is only one minimum, for $b < 0$ a double well is formed. The overall confinement of the double well potential along the splitting direction depends only on the coefficient of the x^4 term (d). By Taylor expanding the potentials created by the RF-beamsplitter and the two-wire setup one finds

$$\frac{d_{\mathrm{RF}}}{d_{2\mathrm{w}}} \approx \left(\frac{B_{\mathrm{bias}}}{B_{\mathrm{Ioffe}}}\right)^2 \tag{7}$$

which is on the order of 10^3 in typical atom chip experiments. This means that the achievable potential modulation is 1000 times stronger in RF designed potentials than in potentials designed with static fields alone.

Fig. 4 compares the RF double well discussed in this paper with a 2-wire setup utilizing the same wire dimensions and atom-chip distance. For a typical separation of 3μm and $B_{\mathrm{bias}} = 30$ G, $B_{\mathrm{Ioffe}} = 1$ G, we obtain $\frac{d_{RF}}{d_{2w}} = 1260$, in good agreement with the approximation (Eq. 7).

In addition, one sees that the parameter characterizing the two wire splitting (the external bias field B_{bias}) has to be stable to a precision of 10^{-5} for controlled splitting, whereas in the case of RF induced potentials the control parameter (the RF field amplitude) changes by a factor two, greatly reducing the effect of technical fluctuations. Altogether this demonstrates that it is significantly simpler to design and control a miniaturized potential by using RF dressed states.

VI. COLLISIONAL STABILITY

A notable feature of the RF induced adiabatic potentials, as applied in our experiments, is that all the involved frequencies, namely the Larmor frequency $\omega_{\mathrm{L}} = \mu \cdot \mathbf{B}/\hbar$, the radio frequency ω_{RF}, and the resulting Rabi frequency Ω_{R}, are of the same order of magnitude ($\omega_{\mathrm{L}} \sim \omega_{\mathrm{RF}} \sim \Omega_{\mathrm{R}}$). In this regime the dressed eigenstates contain contributions of all bare states defined by the static field. Mixtures of different magnetic spin states usually lead to high loss rates for trapped atoms [21, 22]. Nevertheless we observe no additional loss for atoms trapped in RF potentials compared to the static trap for densities up to 10^{15} atoms/cm^3.

We attribute this collisional stability of atoms in the RF dressed states to an argument given in [23, 24] for weakly dressed atoms during RF-evaporation in magnetic traps: The RF-fields introduce a variation of the potential on length scales smaller than the original static trap, but still large compared to the scattering length of the atoms. Two colliding atom reside in the same adiabatic state, consequently they can be regarded to be in the same spin state when they approach each other closely. The RF dressing only rotates the (local) quantization axis, without affecting the collisional properties. Our observations suggest that this argument is still valid in our regime of $\omega_{\mathrm{L}} \sim \omega_{\mathrm{RF}} \sim \Omega_{\mathrm{R}}$.

In contrast to the observations by [8] and [25] we observe no additional heating processes in the RF dressed state potentials.

VII. EVAPORATIVE COOLING

With the long lifetimes, no additional heating, and high collision rates, evaporative cooling to quantum degeneracy in the RF-induced potentials is possible. This is accomplished by applying a sweep of an additional weak RF field tuned to energy differences in the dressed state

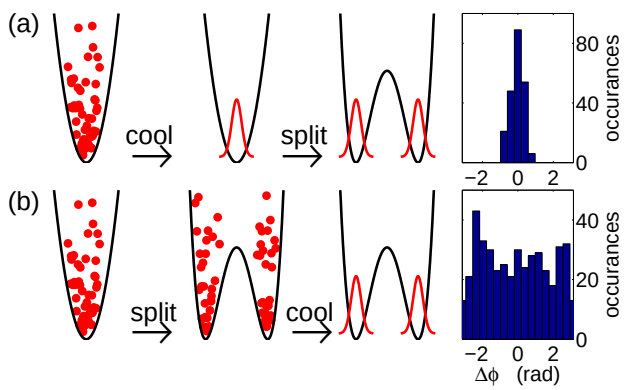

FIG. 5: Comparison of independent and coherently split BECs. (a) For the coherent splitting a BEC is produced in the single well, which is then deformed to a double well. We observe a narrow phase distribution for many repetitions of an interference experiment between these two matter waves, showing that there is a deterministic phase evolution during the splitting. (b) To produce two independent BECs, the double well is formed while the atomic sample is thermal. Condensation is then achieved by evaporative cooling in the dressed state potential. The observed relative phase between the two BECs is completely random, as expected for two independent matter waves.

level scheme. The observed RF induced evaporative cooling is as stable and efficient as in the original magnetic trap.

The ability to cool atomic samples in the RF-double well potential allows us to prepare two fully independent condensates from a split thermal cloud. We compare the relative phase between such BECs with that of coherently split BECs in the same potential. Fig. 5 illustrates the two different experimental sequences. In both cases we start with thermal atoms in the static single well potential. In the case of coherent splitting, the sample is first cooled to degeneracy and then the potential is deformed into a double well by the RF dressing field (Fig. 5a). Alternatively, we apply the RF field first, splitting the thermal cloud, and then cool the two separate samples (Fig. 5b). The height of the potential barrier between the two wells is set to $U \approx 4\ \mu$K, ensuring that the two samples are already separated at temperatures well above the condensation temperature $T_C \approx 0.4\ \mu$K.

We obtain the relative phase ϕ_{rel} between the two BECs from the interference patterns observed in ToF after release from the double well. For the coherently split BECs we observe a narrow gaussian distribution of the relative phase ($\sigma = 0.2rad$) centered around $\phi_{rel} = 0$. The independently created BECs show the expected completely random phase distribution [26, 27].

In future experiments precise control over the coupling of the two 1d condensates with a tunable tunnel barrier between the two wells will allow detailed studies of the coherence dynamics like phase locking, phase diffusion and phase fluctuations and their dependence on the initial state (coherently split or independently created) and the reduced dimensionality of the BECs.

VIII. CONCLUSION

We have presented RF-induced dressed state potentials and illustrated their remarkable features in experiments utilizing a simple and highly integrated setup on an atom chip.

The RF-potentials greatly enhance the flexibility and robustness of atom manipulation. Detailed control over the polarization allows to create internal state dependent potentials with RF coupling. Applying this to the $F = 1, m_F = -1$ and the $F = 2, m_F = 1$ clock states in ^{87}Rb, which have the same magnetic moment $\mu = \mu_B g_F m_F$ but opposite sign g-factors ($g_1 = -g_2$) will enable high precision state dependent manipulation for QIPC applications [28]. Implementation of multi frequency RF fields can additionally enhance the freedom to design potentials [29].

Furthermore we found no adverse effects of RF dressing, neither in the collisional stability and trap loss, nor in heating. This allows the application of RF evaporative cooling and fast and efficient creation of BECs in the dressed state potentials.

The robustness of the RF dressing related to collisional losses opens up new avenues to manipulate the interaction between atoms (molecules) by tuning to molecular states and dressing inside the collision. With the large coupling strength and gradients obtainable on atom chips, the formation of RF and MW induced Feshbach resonances [24] become feasible.

From our experiments we are convinced that RF dressed state potentials with their robustness and flexibility will very quickly become a standard tool for cold atom manipulation comparable to magnetic trapping or optical dipole potentials.

a. ***Acknowledgement*** We would like to thank Thorsten Schumm and Peter Krüger for stimulating discussions and critical reading of the manuscript. The atom chip used in this experiment was fabricated at the Weizman Institut of Science by S. Groth. We acknowledge financial support from the European Union, through the contracts IST-2001-38863 (ACQP), MRTN-CT-2003-505032 (Atom Chips), Integrated Project FET/QIPC "SCALA" , and the Deutsche Forschungsgemeinschaft, contract number SCHM 1599/1-1.

IX. METHODS

b. ***Calculation of the dressed state potentials*** The magnetic fields given in Eq. (2) represent a good approximation of the fields generated by the actual experimental setup which is shown in Fig. 1. For all quantitative calculations presented here we have numerically calculated the magnetic fields. In the course of the latter

we have taken into account the actual layout and dimensions of the wires which essentially result in imperfections of the magnetic quadrupole and inhomogeneities of the RF fields. The Rabi frequency $\Omega_{\rm RF}(\mathbf{r})$ and the dressed state potentials have then been calculated following Refs. [10, 30].

c. ***Experimental Procedure*** We routinely prepare samples of $\sim 3\times10^5$ ^{87}Rb atoms in the F=m$_F$=2 state at a temperature of $\sim 2\mu$K in the chip trap formed by the central Z-wire following our standard procedure [31]. Pure condensates containing between 10^3 and 10^5 atoms are produced by a final stage of evaporative cooling. The number of atoms in the condensate can be adjusted by the end frequency of the final RF cooling ramp.

The distance from the chip surface where the field configuration given in Eq. 2 is realized is 115 μm. At this height residual potential roughness has not been observed with even the most sensitive measurements [32, 33] and is extrapolated to be many orders of magnitude smaller than the chemical potential of the BEC.

The transverse confinement in the static trap can be adjusted by the wire current and the external bias field. The parameters are chosen such that $\omega_\perp = 3$ kHz. The longitudinal confinement is provided by the outer leads of the Z-shaped wires, in addition it can be modified by the U-shaped wires on the side of the three-wire setup (Fig. 1b). For the experiments described here, we used $\omega_\parallel \sim 10$ Hz. The chemical potential μ of the BEC in this trap fulfills $\mu \simeq \hbar\omega_\perp$, so that we are working in the 1D crossover region.

d. ***Imaging the atoms*** The atomic clouds are studied either *in situ* or in time-of-flight by resonant absorption imaging. The diffraction limited resolution of the imaging system is adjusted to have a focal depth compatible with the longitudinal size of the atomic cloud. In the experiments here it was set to ~ 5 μm to allow imaging of 100 μm long clouds.

e. ***RF spectroscopy of dressed state potentials*** The energy difference between different dressed state potentials can be measured by inducing transitions with a weak additional RF field, transferring atoms to untrapped states. This induces trap loss, which is the signature for achieving resonance. The resolution of this method is limited by the chemical potential of the BEC to ~ 2 kHz.

f. ***Evaporative cooling in dressed state potentials*** One can use the loss caused by transitions between dressed state energy levels for evaporative cooling. Unlike for the case of a static magnetic trap not only one but multiple resonance frequencies between the dressed energy levels at which atoms can be transferred to un-trapped states can be identified. We find that the efficiency of the evaporation process differs for these resonances.

[1] C. Cohen-Tannoudji, J. Dupont-Roc, and G. Grynberg, *Atom-Photon Interactions* (Wiley, New York, 1992).

[2] R. Grimm, M. Weidemüller, and Y. B. Ovchinnikov, Adv. At. Mol. Opt. Phys. **42**, 95 (2000).

[3] See atom traps world wide: http://www.uibk.ac.at/exphys/ultracold/atomtraps.html and links therein.

[4] E. Muskat, D. Dubbers, and O. Schärpf, Phys. Rev. Lett. **58**, 2047 (1987).

[5] C. C. Agosta, I. F. Silvera, H. T. C. Stoof, and B. J. Verhaar, Phys. Rev. Lett. **62**, 2361 (1989).

[6] R. J. C. Spreeuw, C. Gerz, L. S. Goldner, W. D. Phillips, S. L. Rolston, C. I. Westbrook, M. W. Reynolds, and I. F. Silvera, Phys. Rev. Lett. **72**, 3162 (1994).

[7] O. Zobay and B. M. Garraway, Phys. Rev. Lett. **86**, 1195 (2001).

[8] Y. Colombe, E. Knyazchyan, O. Morizot, B. Mercier, V. Lorent, and H. Perrin, Europhys. Lett. **67**, 593 (2004).

[9] T. Schumm, S. Hofferberth, L. M. Andersson, S. Wildermuth, S. Groth, I. Bar-Joseph, J. Schmiedmayer, and P. Krüger, Nature Phys. **1**, 57 (2005).

[10] I. Lesanovsky, T. Schumm, S. Hofferberth, L. M. Andersson, P. Krüger, and J. Schmiedmayer, Phys. Rev. A **73**, 033619 (2006).

[11] R. Folman, P. Krüger, J. Schmiedmayer, J. Denschlag, and C. Henkel, Adv. At. Mol. Opt. Phys. **48**, 263 (2002).

[12] D. S. Petrov, G. V. Shlyapnikov, and J. T. M. Walraven, Phys. Rev. Lett. **85**, 3745 (2000).

[13] C. Menotti and S. Stringari, Phys. Rev. A **66**, 043610 (2002).

[14] P. Krüger, X. Luo, M. W. Klein, K. Brugger, A. Haase, S. Wildermuth, S. Groth, I. Bar-Joseph, R. Folman, and J. Schmiedmayer, Phys. Rev. Lett. **91**, 233201 (2003).

[15] D. Cassettari, B. Hessmo, R. Folman, T. Maier, and J. Schmiedmayer, Phys. Rev. Lett. **85**, 5483 (2000).

[16] E. A. Hinds, C. J. Vale, and M. G. Boshier, Phys. Rev. Lett. **86**, 14621465 (2001).

[17] W. Hänsel, J. Reichel, P. Hommelhoff, and T. W. Hänsch, Phys. Rev. A **64**, 063607 (2001).

[18] Y. Shin, C. Sanner, G.-B. Jo, T. A. Pasquini, M. Saba, W. Ketterle, D. E. Pritchard, M. Vengalattore, and M. Prentiss, Phys. Rev. A **72**, 021604 (2005).

[19] J. Stickney and A. Zozulya, Phys. Rev. A **68**, 013611 (2003).

[20] J. D. Davis, Eur. Phys. J. D **18**, 27 (2002).

[21] P. S. Julienne, F. H. Mies, E. Tiesinga, and C. J. Williams, Phys. Rev. Lett. **78**, 1880 (1997).

[22] A. J. Moerdijk and B. J. Verhaar, Phys. Rev. A **53**, R19 (1996).

[23] K.-A. Suominen, E. Tiesinga, and P. S. Julienne, Phys. Rev. A **58**, 3983 (1998).

[24] A. J. Moerdijk, B. J. Verhaar, and T. M. Nagtegaal, Phys. Rev. A **53**, 4343 (1996).

[25] M. White, H. Gao, M. Pasienski, and B. DeMarco (2006), cond-mat/0605393.

[26] Y. Castin and J. Dalibard, Phys. Rev. A **55**, 4330 (1997).

[27] M. R. Andrews, C. G. Townsend, H.-J. Miesner, D. S. Durfee, D. M. Kurn, and W. Ketterle, Science **275**, 637 (1997).

[28] T. Calarco, E. A. Hinds, D. Jaksch, J. Schmiedmayer,

J. I. Cirac, and P. Zoller, Phys. Rev. A **61**, 022304 (2000).
[29] P. W. Courteille, B. Deh, J. Fortagh, A. Günther, S. Kraft, C. Marzok, S. Slama, and C. Zimmermann, J. Phys. B: At. Mol. Opt. Phys. **39**, 1055 (2006).
[30] I. Lesanovsky, S. Hofferberth, J. Schmiedmayer, and P. Schmelcher, physics/0606165 (2006).
[31] S. Wildermuth, P. Krüger, C. Becker, M. Brajdic, S. Haupt, A. Kasper, R. Folman, and J. Schmiedmayer, Phys. Rev. A **69**, 030901(R) (2004).
[32] S. Wildermuth, S. Hofferberth, I. Lesanovsky, E. Haller, L. Andersson, S. Groth, I. Bar-Joseph, P. Krüger, and J. Schmiedmayer, Nature **435**, 440 (2005).
[33] P. Krüger, L. M. Andersson, S. Wildermuth, S. Hofferberth, E. Haller, S. Aigner, S. Groth, I. Bar-Joseph, and J. Schmiedmayer, eprint arXiv:cond-mat/0504686 (2005).